

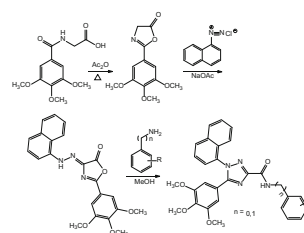
Synthesis, cytotoxicity, and docking study of novel 1-naphthyl-5-aryl-1*H*-1,2,4-triazole-3-carboxamides

Islam Zaki¹ · Mohamed Ramadan² · Mostafa H. Abdelrahman² · Omar M. Aly^{3,4}

Received: 22 October 2016 / Accepted: 30 December 2016
© Springer-Verlag Wien 2017

Abstract A new series of 1-naphthyl-5-aryl-1*H*-1,2,4-triazole-3-carboxamide derivatives were synthesized and structurally proved by ¹H and ¹³C NMR along with high-resolution mass spectrometry. The cytotoxic activity of the newly synthesized compounds was evaluated. Compounds showed a pronounced inhibitory effect against cellular localization of tubulin. Flow cytometric analysis showed that Hep-G2 cells treated indicated a predominated growth arrest at the G2/M-phase compared to that of S-phase. Molecular modeling study using MOE program indicated that most of the target compounds showed good binding with the colchicine-binding site of β -subunit of tubulin with the binding free energy (ΔG) values of about 42 kJ/mol.

Graphical abstract



Keywords Computational chemistry · Structure elucidation · Structural activity relationship · Cytotoxicity · Combretastatin · Tubulin

Introduction

The importance of tubulin and microtubules in chromosome segregation during cell division makes them an attractive target for anticancer drug design, i.e., in the development of antimetabolic agents [1, 2]. Tubulin is the building block of microtubules, which are important in cellular functions such as cell transport, movement and separation of chromosomes during mitosis in addition to the cytoskeleton structure [3]. Several research studies have elucidated at least three distinct binding regions on tubulin. They are the vinca, taxane, and colchicine binding sites. Antimetabolic agents with the capability of binding to the colchicine site of tubulin have received much attention and some of them such as combretastatin A-4 (CA-4) and its water-soluble prodrug CA-4P are undergoing clinical trials as antitumor drugs [4, 5].

CA-4 is the most biologically significant member of *cis*-stilbenes isolated by Pettit and coworkers from a bush

Electronic supplementary material The online version of this article (doi:10.1007/s00706-016-1910-8) contains supplementary material, which is available to authorized users.

✉ Mohamed Ramadan
elbashamohammed@yahoo.com

¹ Faculty of Pharmacy, Organic Chemistry Department, Port Said University, Port Said, Egypt

² Faculty of Pharmacy, Organic Chemistry Department, Al-Azhar University, Assuit, Egypt

³ Faculty of Pharmacy, Medicinal Chemistry Department, Minia University, Minia, Egypt

⁴ College of Clinical Pharmacy, Pharmaceutical Chemistry Department, AlBaha University, AlBaha, Saudi Arabia

willow tree *Combretum caffrum* in South Africa. This compound was found to be a potent antiproliferative agent against a broad spectrum of cancer cell lines including multi-drug-resistant cells [6].

Structure–activity relationship studies on CA-4 derivatives have established that pharmacophore structure for binding to tubulin is the *cis*-oriented two ethenyl-bridged aromatic rings with one of them bearing 3,4,5-trimethoxy substituents [7]. However, due to the poor aqueous solubility and relative chemical instability of many *cis*-stilbenes, 5-membered heterocycles including triazoles [8, 9] have been widely explored as alternative bridging groups. Also, 3,4,5-trimethoxyaryl ring-A is generally considered to be essential for biological activity. Since the trimethoxyaryl ring-A is present in several other antimetabolic agents (colchicine, podophyllotoxin, and steganacin) that also bind at the colchicine-binding site, it may have been presumed to be a privileged scaffold important for effective binding. On the other hand, it has been reported that this is not the case and equivalent potency can be attained via the change of the ring-A in *cis*-stilbene analogs [10, 11] (Fig. 1).

Here, the synthesis and evaluation of the cytotoxicity of combretastatin analogs bearing triazole ring that replaced the ethylene bridge of the natural CA-4 were done. Furthermore, to study the full structure–activity relationship of the ring-A and ring-B on the triazole ring, we investigated the effect of 3,4,5-trimethoxyphenyl functionality on cytotoxic activity. Therefore, we prepared compounds containing trimethoxy, dimethoxy, monomethoxy, and unsubstituted ring-A, alongside replacement of ring-B with more lipophilic group, e.g., 1-naphthyl moiety, since the lipophilicity is important in protein binding.

The antitumor activity of each compound was tested *in vitro* on two different human cancer cell lines in addition to the anticancer screening done by the NCI, USA, for the selected compounds against a panel of 60 cell lines derived from nine different types of cancers including, leukemia, melanoma, lung, colon, CNS, ovarian, renal, prostate, and breast cancers. Also, the mechanism of action of the promising compounds was investigated. Moreover, tubulin polymerization inhibitory activity expressed in the localization of tubulin was explored in Hep-G2 cell line after

treating with selected promising compounds as indicated by ELISA through immunofluorescence labeling and analysis under ApoTome fluorescence microscope. Also, to explore the alteration in the cell cycle phases after treatment with the active cytotoxic compounds **4c** and **7k**, the cells were subjected to flow cytometry analysis. Furthermore, molecular modeling studies of some of the prepared compounds with the colchicine-binding site of β -tubulin were also performed.

Results and discussion

Chemistry

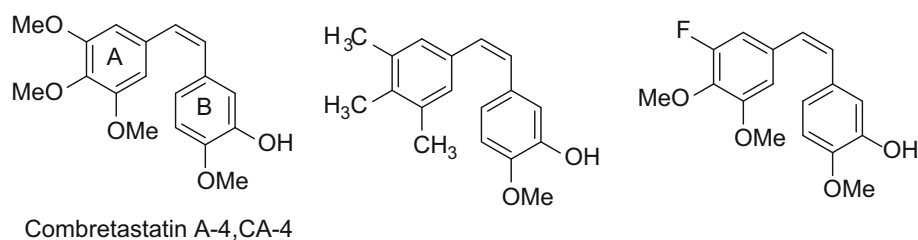
The reaction sequences employed for synthesis of the target compounds are shown in Scheme 1. Key starting compound, 2-(un)substituted benzamido]acetic acid derivatives **1a–1d**, were prepared in good yield of about 85% by the reaction of glycine with benzoyl chloride derivatives in 10% NaOH [12]. Heating of compounds **1a–1d** with acetic anhydride afforded the corresponding compounds **2a–2d**. The key intermediate, 4-(1-naphthyl)-hydrazono-2-[(un)substituted aryl]-2-oxazolin-5-one derivatives **3a–3d** were prepared by diazotization of 1-naphthylamine followed by reaction with the active methylene compounds **2a–2d** [13, 14]. IR spectrum of intermediate **3a** showed a weak and broad band at 3615–3300 cm^{-1} . The broadening of the NH stretching band indicates the effect of possible intramolecular hydrogen bonding with the nitrogen atom of oxazolinone. Strong stretching bands occurred at 1794 (C=O) of the lactone, bands at 1626 (C=N), 1229 (C–O–C), and 1600–1585 (C=C) cm^{-1} .

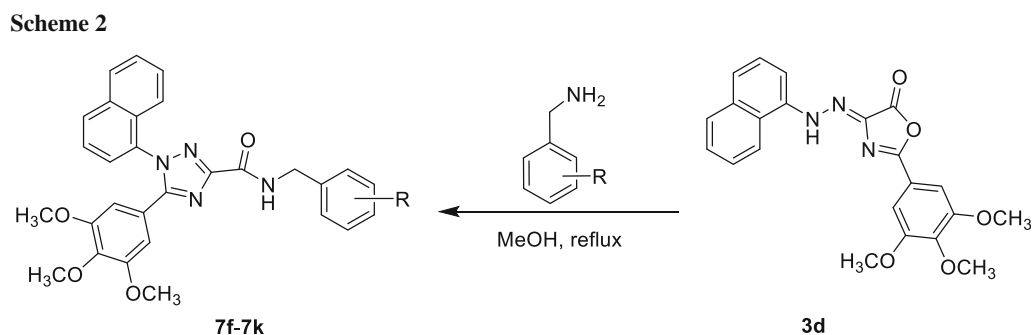
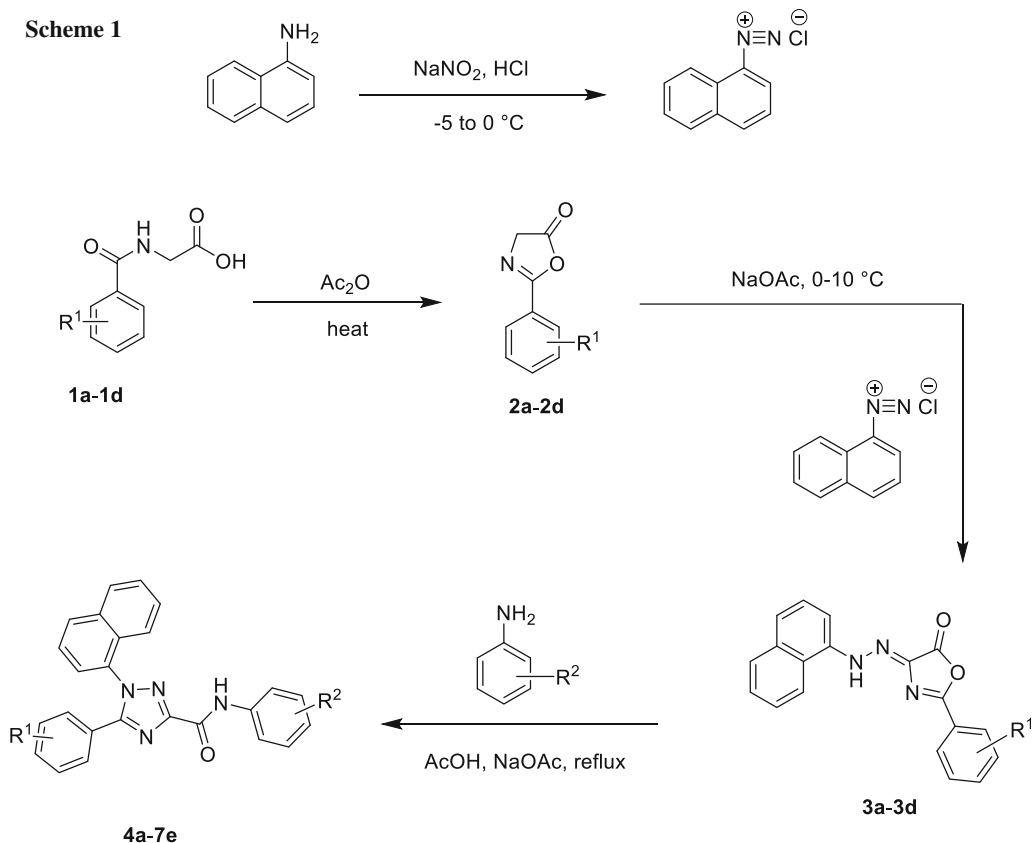
Rearrangement of compounds **3a–3d** upon treatment with different primary aromatic amines in acidic medium afforded the target anilide derivatives **4a–7e**, while the reaction of compound **3d** with substituted benzylamine in methanol afforded the compounds **7f–7k** (Schemes 1, 2).

Antitumor activity against two different human cancer cell lines

Using MTT assay, the triazole derivatives **4a–7k** were tested for their antitumor activity on two cancer cell lines, hepatocellular carcinoma and leukemia HL-60 cell lines,

Fig. 1 Structure of naturally occurring CA-4 and its analogs





using CA-4 as a reference compound. The effect of the tested compounds on the viability of different human cancer cell lines was studied after 48 h of incubation. Treatment of Hep-G2 cells and leukemia HL-60 cells with gradual concentrations of different compounds revealed that compounds **4c**, **6a**, and **7e**, **7f**, **7i**, **7k** possessed good cytotoxic effect against two cell lines as concluded from their IC_{50} values, as shown in Table 1.

Also, the selected compounds were screened for their anticancer activity at NIH, Bethesda, Maryland, USA, under the drug discovery program of NCI according to

the procedure suggested by Boyd. The selected compounds were tested at a single concentration of $10\ \mu\text{M}$. Results for each test agent are reported as the percent growth of the test cells when treated with the untreated control cells (Table 2). The results showed that compound **7c** exhibited promising anticancer activity. Compound **7c** with NSC code No. D-789118 was active against four cancer cell lines: Leukemia: HL-60(TB), RPMI-8226; Colon Cancer: HCT-15; Renal Cancer: UO-31, while compounds **4d-4e**, **5a**, **5b**, and **6e** showed moderate activities.

Table 1 Collective calculated IC₅₀ (μM) from linear equation of dose–response curve for each tested sample against liver carcinoma Hep-G2 cells and leukemia HL-60 cells

Compound	R ¹	R ²	Collective calculated IC ₅₀ /μM	
			Liver carcinoma Hep-G2 cells	Leukemia HL-60 cells
4a	H	2-OCH ₃	>100	>100
4b	H	3-OCH ₃	74.53	>100
4c	H	3,4-OCH ₃	<u>36.75</u>	>100
4d	H	3,4,5-OCH ₃	>100	>100
4e	H	3,5-F	57.66	>100
5a	4-OCH ₃	2-OCH ₃	>100	>100
5b	4-OCH ₃	3-OCH ₃	72.89	72.89
5c	4-OCH ₃	3,4-OCH ₃	82.26	42.71
5d	4-OCH ₃	3,4,5-OCH ₃	55.71	89.49
5e	4-OCH ₃	3,5-F	89.49	>100
6a	3,4-OCH ₃	2-OCH ₃	80.18	<u>32.44</u>
6b	3,4-OCH ₃	3-OCH ₃	>100	>100
6c	3,4-OCH ₃	3,4-OCH ₃	92.41	>100
6d	3,4-OCH ₃	3,4,5-OCH ₃	>100	>100
6e	3,4-OCH ₃	3,5-F	>100	>100
7a	3,4,5-OCH ₃	2-OCH ₃	>100	<u>19.53</u>
7b	3,4,5-OCH ₃	3-OCH ₃	>100	>100
7c	3,4,5-OCH ₃	3,4-OCH ₃	>100	65.23
7d	3,4,5-OCH ₃	3,4,5-OCH ₃	>100	68.24
7e	3,4,5-OCH ₃	3,5-F	>100	<u>46.88</u>
7f	3,4,5-OCH ₃	2-OCH ₃	<u>42.24</u>	78.63
7g	3,4,5-OCH ₃	3-OCH ₃	>100	94.00
7h	3,4,5-OCH ₃	3,4-OCH ₃	>100	65.19
7i	3,4,5-OCH ₃	3,5-F	>100	<u>22.77</u>
7j	3,4,5-OCH ₃	3-CH ₃	>100	>100
7k	3,4,5-OCH ₃	H	<u>24.7</u>	34.58

Immunofluorescence localization of tubulin in liver cancer cells

The effect of triazoles **4a**, **4e**, **5d**, **6a**, **7f**, **7k** and CA-4 on tubulin localization was also investigated to confirm this hypothesis. Hep-G2 cells were tested with 25 μM of each compound for 48 h, and then submitted to immunofluorescence labeling and analysis under fluorescence microscope. The treatment of hepatocellular carcinoma Hep-G2 cells revealed that compounds **4c**, **5d**, and **7k** showed good inhibitory effect on cellular tubulin formation (about 65% of that of the original control tubulin) (Fig. 2), while compound **7f** showed moderate inhibitory activity as concluded from the inhibition of the fluorescence intensity, while compound **6a** showed a mild degree tubulin polymerization inhibitory activity.

Cell-cycle analysis

A hallmark of antitubulin agents is their ability to arrest cycling cells in the G2/M-phase of the cell cycle. To determine whether the above cytotoxic effects were due to

interruption of the functioning of cellular microtubules, Hep-G2 cells were treated with compounds **4c** and **7k** at concentration 25 μM and were investigated using flow cytometry. The cell-cycle analyses were performed at different compound concentrations. The analysis indicated that Hep-G2 cells treated with **4c** showed a predominated growth arrest at the S- and G2/M-phases ($p < 0.01$) as compared with control cells, where the S-phase progression of Hep-G2 cells was considerably delayed. Hep-G2 cells treated with **7k** showed a predominated growth arrest at the G2/M-phase higher than that of S-phase ($p < 0.01$) as compared with control cells, where the G2/M-phase progression of Hep-G2 cells was considerably delayed (Fig. 3).

Molecular docking

Docking calculations were carried out on 1SA0 protein model obtained from Protein Data Bank. Inspection of the colchicines-binding site revealed that colchicine site is mostly buried in the intermediate domain of the β subunit. Colchicine also interacts with loop T5 of the neighboring β subunit.

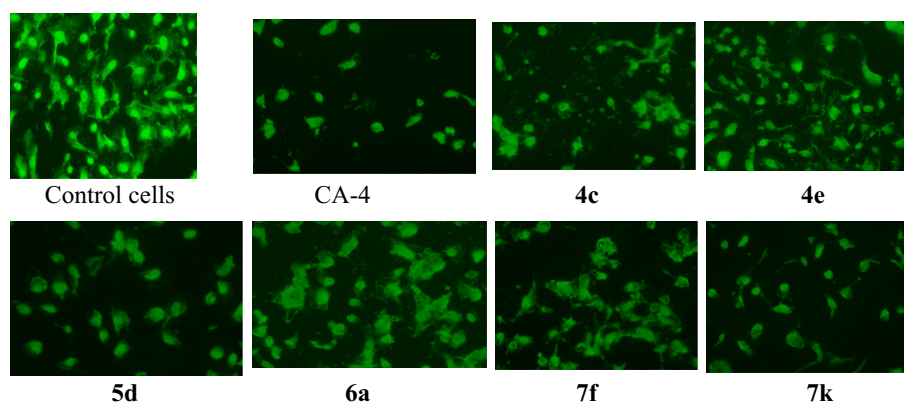
Table 2 Sixty cell line in vitro anticancer screening data of compounds **4d**, **4e**, **5a**, **5b**, **6e**, and **7c**

Subpanel tumor cell lines	Growth % (G%)					
	4d	4e	5a	5b	6e	7c
Leukemia						
CCRF-CEM	90.18	67.40	101.01	84.64	97.77	–
HL-60(TB)	67.93	–	76.34	69.57	85.28	10.01
K-562	55.22	–	80.73	64.31	80.76	35.37
MOLT-4	70.26	–	67.42	51.67	77.25	–
RPMI-8226	72.91	94.10	66.69	61.65	66.91	11.62
SR	60.30	–	64.26	74.97	77.84	33.13
Non-small cell lung cancer						
A549/ATCC	73.84	89.57	77.01	64.92	88.92	50.63
EKVX	62.59	73.84	77.83	64.76	81.70	44.55
HOP-62	64.59	86.93	93.16	79.22	79.39	42.10
HOP-92	72.74	106.46	73.89	92.95	98.06	46.41
NCI-H226	77.32	86.50	83.35	73.77	77.36	44.94
NCI-H23	74.53	87.30	82.47	69.73	76.70	45.37
NCI-H322 M	72.89	63.31	73.80	57.05	69.27	44.82
NCI-H460	77.34	97.27	87.07	78.33	91.61	49.61
NCI-H522	62.35	77.66	55.26	46.15	59.32	21.77
Colon cancer						
COLO 205	85.99	110.38	92.14	83.76	97.21	37.10
HCC-2998	98.25	103.08	93.42	102.25	98.44	47.40
HCT-116	54.01	73.98	76.38	50.84	58.28	25.86
HCT-15	65.78	79.95	65.62	72.38	73.28	14.50
HT29	72.07	104.68	78.85	74.53	101.28	29.99
KM12	74.84	82.86	81.87	78.78	84.71	41.26
SW-620	79.28	93.96	93.48	75.87	92.95	61.54
CNS cancer						
SF-268	86.40	82.42	86.55	74.50	86.87	58.56
SF-295	83.05	94.54	90.08	78.04	85.84	52.62
SF-539	93.73	91.75	87.32	89.60	95.87	34.98
SNB-19	81.57	84.30	89.27	86.79	99.84	52.34
SNB-75	54.77	68.43	69.71	66.28	79.84	24.43
U251	88.27	95.01	91.88	72.52	85.95	52.37
Melanoma						
LOX IMVI	77.86	88.44	76.18	51.97	81.51	25.23
MALME-3 M	81.47	67.42	77.27	74.19	82.47	52.83
M14	75.05	85.23	82.25	79.54	77.80	48.01
MDA-MB-435	44.37	99.38	92.87	91.84	89.97	47.43
SK-MEL-2	68.08	90.96	76.61	80.58	88.55	43.74
SK-MEL-28	89.26	87.37	82.91	95.20	96.40	55.37
SK-MEL-5	89.45	97.83	74.65	90.31	85.34	32.44
UACC-257	96.93	94.95	92.31	92.60	103.49	57.49
UACC-62	72.17	75.36	71.80	74.10	86.51	30.99
Ovarian cancer						
IGROV1	64.40	68.57	68.74	45.53	58.90	22.92
OVCAR-3	81.36	85.37	70.22	60.68	70.09	27.70
OVCAR-4	67.20	87.85	66.01	54.35	73.84	45.46
OVCAR-5	84.50	88.93	94.29	80.34	83.80	56.11

Table 2 continued

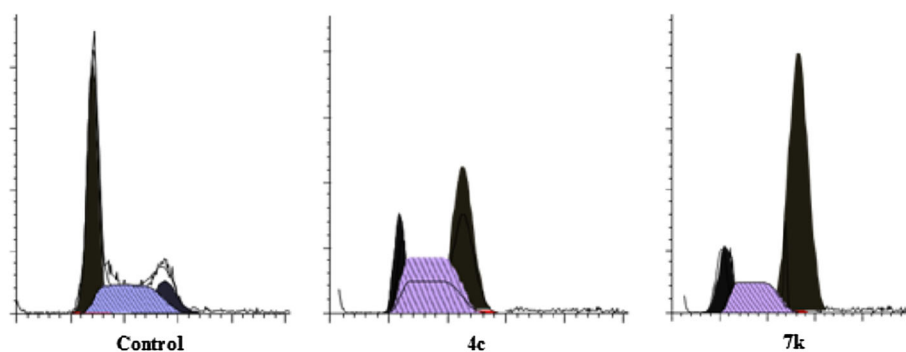
Subpanel tumor cell lines	Growth % (G%)					
	4d	4e	5a	5b	6e	7c
OVCAR-8	87.37	100.19	92.11	88.22	92.29	52.46
NCI/ADR-RES	76.30	84.04	85.77	71.15	86.51	35.25
SK-OV-3	65.83	90.01	84.73	77.98	79.48	38.30
Renal cancer						
786-0	79.51	93.84	104.56	85.95	83.74	31.75
A498	83.01	102.67	98.87	87.43	94.63	42.60
ACHN	75.26	86.37	69.50	52.64	78.40	30.55
CAKI-1	70.72	80.44	73.30	59.95	65.11	20.07
RXF 393	84.84	92.51	98.90	82.08	101.26	66.13
SN12C	85.02	89.88	87.27	76.53	82.53	52.87
TK-10	76.89	89.29	101.04	88.19	101.39	44.76
UO-31	37.88	46.88	41.26	24.27	38.12	6.34
Prostate cancer						
PC-3	59.16	83.18	56.77	55.93	65.96	39.81
DU-145	106.69	106.13	98.63	90.01	109.21	70.35
Breast cancer						
MCF7	59.27	72.83	64.26	57.95	69.61	26.23
MDA-MB-231/ATCC	68.38	83.50	48.98	34.48	61.89	26.96
HS 578T	90.89	89.73	85.82	89.96	91.83	23.35
BT-549	65.77	91.16	91.37	83.03	78.08	46.30
T-47D	47.70	66.49	67.16	61.26	76.06	50.32
MDA-MB-468	80.99	101.89	90.48	93.93	94.15	46.38

Fig. 2 Fluorescence intensity of tubulin localization in Hep-G2 cells after treatment with combretastatin A-4, compounds **4c**, **4e**, **5d**, **6a**, **7f**, and **7k** at concentration of 25 μ M for 48 h compared to control cells



The tested compounds **4c**, **5d**, **6d**, and **7c** showed similar binding to colchicines and inhibition of tubulin protein of 1SA0. The results of interaction energies with tubulin protein of 1SA0 are shown in Table 3. Molecular docking simulation of compound **4c** into tubulin protein active site was done. It goes stabilized at the colchicine-binding site of tubulin by one H-bond interaction between oxygen in the carbonyl group of the ligand and Met-259 (Fig. 4). Also, molecular docking simulation of compound **5d** into tubulin protein of 1SA0 revealed several molecular

interactions considered to be responsible for the observed affinity: two H-bond interactions, between oxygen in carbonyl group of the ligand and Lys-352 and Thr-353, two H-bond interactions, between carbon of trisubstituted-phenyl and naphthyl in the ligand and Thr-353 and Leu-255, respectively, and only one π -H bond interaction between the triazole ring of the ligand and Leu-248. Compound **6d** showed one H-bond interaction between oxygen in carbonyl group of the ligand and Met-259; in addition, one π -H bond interaction between the naphthyl

Fig. 3 Cell-cycle analysis of compound **4c** and **7k** (25 μ M) compared to control**Table 3** Interactions of compounds **4c**, **5d**, **6d**, and **7c** with 1SA0 tubulin protein

Compound	Ligand	Receptor	Interaction	Distance	$\Delta E/kJ\ mol^{-1}$
CA 4	C 19	SD Met 259 (B)	H-donor	4.07	-46.8870
	C 18	SD Met 259 (B)	H-donor	3.60	
4c	O 20	SD Met 259 (B)	H-donor	3.20	-42.1803
5d	C 37	N Thr 353 (B)	H-donor	3.16	-51.0101
	C 55	N Leu 255 (B)	H-donor	2.86	
	O 24	C Lys 352 (B)	H-acceptor	2.76	
	O 24	N Thr 353 (B)	H-acceptor	2.80	
	5-ring	CD ₁ Leu 248(B)	π -H	3.94	
6d	O 28	SD Met 259 (B)	H-donor	2.94	-40.7128
	6-ring	CE Lys 352 (B)	π -H	4.10	
7c	5-ring	CE Lys 352 (B)	π -H	4.01	-42.2309

ring of the ligand and Lys 352 (Fig. 4). Also, compound **7c** showed π -H bond interaction between the triazole ring of the ligand and Lys-352.

Experimental

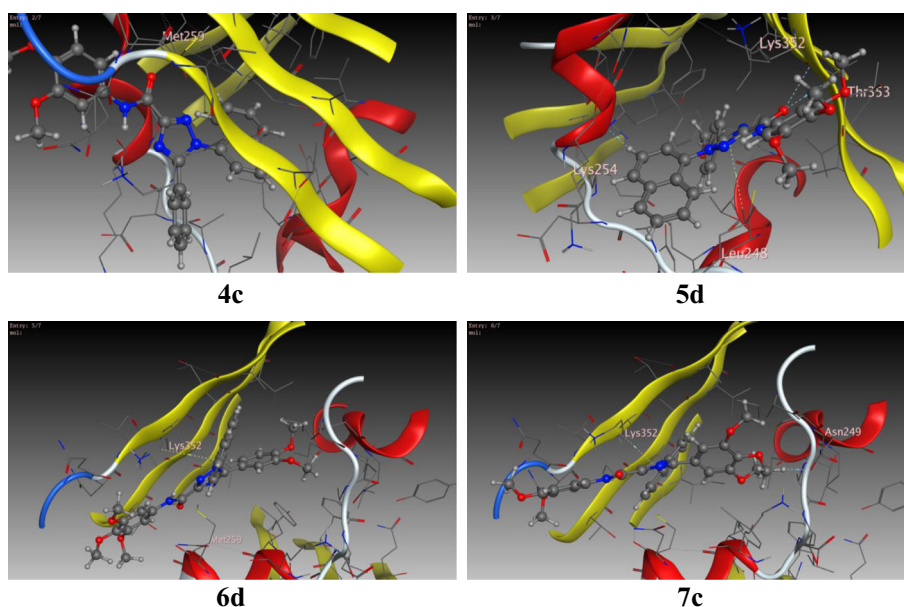
Melting points were determined on an electrothermal melting point apparatus (Stuart Scientific, Model SMP3, UK). The progress of reactions and the purity of the prepared compounds were monitored by thin-layer chromatography (TLC) using Merck 9385 pre-coated aluminum plate silica gel (Kieselgel 60) 5 cm \times 20 cm plates with a layer thickness of 0.2 mm. The spots were detected by exposure to UV-lamp at $\lambda = 254$ nm. NMR spectra were taken using Varian Unity INOVA 400 MHz spectrometers for proton and carbon. All numbers referring to NMR data obtained are in ppm at Aberdeen University, UK. High-resolution mass spectroscopic data were obtained using the EPSRC Mass Spectrometry Centre in Swansea and Thermo Instruments MS system (LTQ XL/LTQ Orbitrap Discovery) coupled to a Thermo Instruments HPLC system (Accela PDA detector, Accela PDA

autosampler and Pump) at University of Aberdeen, UK. Reagents used for synthesis were purchased from Sigma-Aldrich and Merck. All solvents were obtained from commercial suppliers and used without further purification. The starting material 3,4,5-trimethoxyhippuric acid was synthesized according to reported procedures [12].

4-(1-Naphthyl)-hydrazono-2-aryl-2-oxazolin-5-ones **3a-3d**

A mixture of benzoyl glycines **1a-1d** (0.02 mol) and 75 cm³ acetic anhydride was gently heated until a clear solution **2a-2d** was obtained. The resulting solution (A) was cooled in an ice bath before treating with a solution (B) of naphthalene diazonium chloride prepared as follows: 3.2 g 1-naphthylamine (0.02 mol) was mixed with 5 cm³ H₂O and 6 cm³ conc. HCl. The mixture was cooled in an ice bath and an aqueous solution of 1.38 g NaNO₂ (0.02 mol) was introduced dropwise and the resulting mixture was stirred for further 30 min. Freshly prepared crude solution (A) was added dropwise in the presence of 1.64 g anhydrous sodium acetate (0.02 mol) and the stirring was continued for further 2 h at 0 °C. The resulting crude precipitate was filtered, washed with water, and dried [13, 14].

Fig. 4 3D representation of docking of compounds **4c**, **5d**, **6d**, and **7c** into the 1SA0 tubulin protein



4-[2-(Naphthalen-1-yl)hydrazono]-2-phenyloxazol-5(4H)-one (**3a**, C₁₉H₁₃N₃O₂)

Red powder (3.9 g, 55% yield); m.p.: 61–63 °C (ethanol); IR (KBr): $\bar{\nu}$ = 1794 (C=O), 1626 (C=N), 1585 (C=C), 1229 (C–O–C) cm⁻¹; ¹H NMR (60 MHz, CDCl₃): δ = 9.69 (s, 1H, NH), 8.61–7.04 (m, 12H, Ar–H) ppm.

2-(4-Methoxyphenyl)-4-[2-(naphthalen-1-yl)hydrazono]oxazol-5(4H)-one (**3b**, C₂₀H₁₅N₃O₃)

Red powder (2.8 g, 40% yield); m.p.: 55–57 °C (ethanol); IR (KBr): $\bar{\nu}$ = 1795 (C=O), 1630 (C=N), 1520 (C=C), 1230 (C–O–C) cm⁻¹; ¹H NMR (60 MHz, CDCl₃): δ = 9.09 (s, 1H, NH), 8.04–6.72 (m, 11H, Ar–H), 3.73 (s, 3H, OCH₃) ppm.

2-(3,4-Dimethoxyphenyl)-4-[2-(naphthalen-1-yl)hydrazono]oxazol-5(4H)-one (**3c**, C₂₁H₁₇N₃O₄)

Red powder (2.9 g, 38% yield); m.p.: 51–53 °C (ethanol); IR (KBr): $\bar{\nu}$ = 1792 (C=O), 1627 (C=N), 1524 (C=C), 1218 (C–O–C) cm⁻¹; ¹H NMR (60 MHz, CDCl₃): δ = 9.02 (s, 1H, NH), 8.05–6.66 (m, 10H, Ar–H), 3.77 (s, 3H, OCH₃), 3.47 (s, 3H, OCH₃) ppm.

4-[2-(Naphthalen-1-yl)hydrazono]-2-(3,4,5-trimethoxyphenyl)oxazol-5(4H)-one (**3d**, C₂₂H₁₉N₃O₅)

Red powder (4.2 g, 52% yield); m.p.: 70–72 °C (ethanol); IR (KBr): $\bar{\nu}$ = 1797 (C=O), 1634 (C=N), 1512 (C=C), 1215 (C–O–C) cm⁻¹; ¹H NMR (60 MHz, CDCl₃): δ = 9.08 (s, 1H, NH), 8.04–6.68 (m, 9H, Ar–H), 3.79 (s, 3H, OCH₃), 3.50 (s, 6H, 2-OCH₃) ppm.

1-(Naphthalen-1-yl)-5-(substituted aryl)-1H-1,2,4-triazole-3-carboxamides

Method A (**4a–7e**): A mixture of **3** (0.01 mol), appropriate primary aromatic amine (0.01 mol) in 50 cm³ acetic acid,

and 1.5 g anhydrous sodium acetate (0.018 mol) was refluxed for 2 h. The mixture was cooled, poured into ice-cold water. The formed precipitate was filtered, dried, and crystallized from appropriate solvent.

Method B (**7f–7k**): A mixture of **4d** (0.01 mol) and appropriate primary benzyl amine (0.01 mol) was refluxed in 50 cm³ methanol for 1 h. After cooling the reaction mixture, the solvent was evaporated under reduced pressure and the residue was recrystallized from ethylacetate/hexane mixtures.

N-(2-Methoxyphenyl)-1-(naphthalen-1-yl)-5-phenyl-1H-1,2,4-triazole-3-carboxamide (**4a**, C₂₆H₂₁N₄O₂)

Brown crystals (272 mg, 68% yield); m.p.: 95–97 °C (ethanol); IR (KBr): $\bar{\nu}$ = 3315 (NH), 1691 (C=O), 1595 (C–N) cm⁻¹; ¹H NMR (400 MHz, CDCl₃): δ = 9.69 (s, 1H, NH), 8.64 (dd, *J* = 7.9, 1.7 Hz, 1H, Ar–H), 8.05 (d, *J* = 8.2 Hz, 1H, Ar–H), 8.01 (d, *J* = 8.1 Hz, 1H, Ar–H), 7.63–7.43 (m, 7H, Ar–H), 7.35–7.29 (m, 1H, Ar–H), 7.25–7.18 (m, 2H, Ar–H), 7.16–7.08 (m, 1H, Ar–H), 7.08–6.99 (m, 1H, Ar–H), 6.94 (dd, *J* = 8.1, 1.5 Hz, 1H, Ar–H), 3.94 (s, 3H, OCH₃) ppm; ¹³C NMR (101 MHz, CDCl₃): δ = 157.2, 156.7, 156.7, 130.8, 130.5, 129.4, 129.2, 128.5, 128.4, 128.3, 128.1, 127.3, 127.2, 126.6, 125.6, 125.1, 124.2, 122.5, 121.2, 120.3, 109.9, 55.9 ppm; HRMS: *m/z* calcd for C₂₆H₂₁N₄O₂ ([M+H]⁺) 421.1659, found 421.1660.

N-(3-Methoxyphenyl)-1-(naphthalen-1-yl)-5-phenyl-1H-1,2,4-triazole-3-carboxamide (**4b**, C₂₆H₂₁N₄O₂)

Red crystals (312 mg, 78% yield); m.p.: 90–92 °C (ethanol); IR (KBr): $\bar{\nu}$ = 3331 (NH), 1691 (C=O), 1589 (C–N) cm⁻¹; ¹H NMR (400 MHz, CDCl₃): δ = 9.05 (s,

1H, NH), 8.10 (d, $J = 8.2$ Hz, 1H, Ar-H), 7.98 (d, $J = 8.2$ Hz, 1H, Ar-H), 7.65–7.42 (m, 8H, Ar-H), 7.38–7.17 (m, 5H, Ar-H), 6.73 (ddd, $J = 7.4, 2.5, 2.0$ Hz, 1H, Ar-H), 3.85 (s, 3H, OCH₃) ppm; ¹³C NMR (101 MHz, CDCl₃): $\delta = 160.4, 157.0, 156.9, 138.8, 134.4, 134.4, 131.1, 130.8, 129.9, 129.5, 128.8, 128.5, 128.5, 128.3, 127.4, 126.6, 125.7, 125.3, 122.6, 112.3, 110.8, 105.7, 55.5$ ppm; HRMS: m/z calcd for C₂₆H₂₁N₄O₂ ([M+H]⁺) 421.1659, found 421.1649.

N-(3,4-Dimethoxyphenyl)-1-(naphthalen-1-yl)-5-phenyl-1*H*-1,2,4-triazole-3-carboxamide (**4c**, C₂₇H₂₃N₄O₃)

Orange crystals (292 mg, 68% yield); m.p.: 108–110 °C (methanol); IR (KBr): $\bar{\nu} = 3341$ (NH), 1690 (C=O), 1585 (C–N) cm⁻¹; ¹H NMR (400 MHz, CDCl₃): $\delta = 8.99$ (s, 1H, NH), 8.07 (d, $J = 8.4$ Hz, 1H, Ar-H), 7.96 (d, $J = 8.4$ Hz, 1H, Ar-H), 7.62–7.45 (m, 8H, Ar-H), 7.36–7.30 (m, 1H, Ar-H), 7.27–7.18 (m, 3H, Ar-H), 6.87 (d, $J = 8.7$ Hz, 1H, Ar-H), 3.93 (s, 3H, OCH₃), 3.89 (s, 3H, OCH₃) ppm; ¹³C NMR (101 MHz, CDCl₃): $\delta = 157.1, 156.8, 149.3, 146.2, 134.4, 134.4, 131.2, 131.1, 130.7, 129.3, 128.6, 128.3, 128.1, 127.4, 126.6, 125.7, 125.3, 122.6, 112.1, 111.5, 104.9, 56.3, 56.1$ ppm; HRMS: m/z calcd for C₂₇H₂₃N₄O₃ ([M+H]⁺) 451.1765, found 451.1652.

1-(Naphthalen-1-yl)-5-phenyl-*N*-(3,4,5-trimethoxyphenyl)-1*H*-1,2,4-triazole-3-carboxamide (**4d**, C₂₈H₂₈N₄O₄)

Brown crystals (300 mg, 78% yield); m.p.: 128–130 °C (ethanol); IR (KBr): $\bar{\nu} = 3340$ (NH), 1691 (C=O), 1592 (C–N) cm⁻¹; ¹H NMR (400 MHz, CDCl₃): $\delta = 9.00$ (s, 1H, NH), 8.05 (d, $J = 8.2$ Hz, 1H, Ar-H), 7.98 (d, $J = 8.2$ Hz, 1H, Ar-H), 7.61–7.43 (m, 7H, Ar-H), 7.36–7.29 (m, 1H, Ar-H), 7.25–7.17 (m, 2H, Ar-H), 7.09 (s, 2H, Ar-H), 3.89 (s, 6H, 2×OCH₃), 3.84 (s, 3H, OCH₃) ppm; ¹³C NMR (101 MHz, CDCl₃): $\delta = 157.2, 156.9, 153.5, 135.0, 134.4, 134.3, 133.7, 131.1, 130.8, 129.4, 128.8, 128.7, 128.5, 128.3, 127.4, 126.5, 125.7, 125.2, 122.5, 97.8, 61.1, 56.3$ ppm; HRMS: m/z calcd for C₂₈H₂₈N₄O₄ ([M + H]⁺) 481.1870, found 481.1861.

N-(3,5-Difluorophenyl)-1-(naphthalen-1-yl)-5-phenyl-1*H*-1,2,4-triazole-3-carboxamide (**4e**, C₂₅H₁₇F₂N₄O)

Brown crystals (292 mg, 72% yield); m.p.: 106–108 °C (ethanol); IR (KBr): $\bar{\nu} = 3351$ (NH), 1691 (C=O), 1589 (C–N) cm⁻¹; ¹H NMR (400 MHz, CDCl₃): $\delta = 9.14$ (s, 1H, NH), 8.06 (d, $J = 8.2$ Hz, 1H, Ar-H), 7.98 (d, $J = 8.2$ Hz, 1H, Ar-H), 7.62–7.31 (m, 10H, Ar-H), 7.25–7.19 (m, 2H, Ar-H), 6.62 (m, 1H, Ar-H) ppm; ¹³C NMR (101 MHz, CDCl₃): $\delta = 164.5, 164.3, 162.1, 161.9, 157.1, 156.9, 156.3, 134.2, 134.0, 130.9, 130.7, 129.2, 128.7, 128.2, 127.3, 126.2, 125.5, 125.1, 122.2, 102.8, 99.9$ ppm; HRMS: m/z calcd for C₂₅H₁₇F₂N₄O ([M+H]⁺) 427.1365, found 427.1356.

N-(2-Methoxyphenyl)-5-(4-methoxyphenyl)-1-(naphthalen-1-yl)-1*H*-1,2,4-triazole-3-carboxamide

(**5a**, C₂₇H₂₂N₄O₃)

Orange crystals (274 mg, 70% yield); m.p.: 121–123 °C (methanol); IR (KBr): $\bar{\nu} = 3339$ (NH), 1694 (C=O), 1589 (C–N) cm⁻¹; ¹H NMR (400 MHz, CDCl₃): $\delta = 8.99$ (s, 1H, NH), 8.06 (d, $J = 8.3$ Hz, 1H, Ar-H), 7.98 (d, $J = 8.3$ Hz, 1H, Ar-H), 7.61–7.45 (m, 8H, Ar-H), 7.36–7.31 (m, 1H, Ar-H), 7.25–7.17 (m, 3H, Ar-H), 6.87 (d, $J = 8.6$ Hz, 1H, Ar-H), 3.93 (s, 3H, OCH₃), 3.89 (s, 3H, OCH₃) ppm; ¹³C NMR (101 MHz, CDCl₃): $\delta = 157.1, 156.8, 149.3, 146.2, 134.6, 134.4, 131.2, 131.1, 130.7, 129.5, 128.8, 128.6, 128.5, 128.3, 127.4, 126.6, 125.7, 125.3, 122.6, 112.1, 111.5, 104.9, 56.3, 56.1$ ppm; HRMS: m/z calcd for C₂₇H₂₂N₄O₃ ([M+H]⁺) 451.1765, found 451.1762.

N-(3-Methoxyphenyl)-5-(4-methoxyphenyl)-1-(naphthalen-1-yl)-1*H*-1,2,4-triazole-3-carboxamide

(**5b**, C₂₇H₂₃N₄O₃)

Yellow crystals (313 mg, 80% yield); m.p.: 116–118 °C (methanol); IR (KBr): $\bar{\nu} = 3339$ (NH), 1690 (C=O), 1589 (CN) cm⁻¹; ¹H NMR (400 MHz, CDCl₃): $\delta = 9.04$ (s, 1H, NH), 8.06 (d, $J = 8.3$ Hz, 1H, Ar-H), 7.98 (d, $J = 8.3$ Hz, 1H, Ar-H), 7.73–7.43 (m, 7H, Ar-H), 7.43–7.35 (m, 2H, Ar-H), 7.29 (m, 2H, Ar-H), 6.72 (m, 2H, Ar-H), 3.84 (s, 3H, OCH₃), 3.73 (s, 3H, OCH₃) ppm; ¹³C NMR (101 MHz, CDCl₃): $\delta = 161.4, 160.3, 157.0, 156.7, 138.8, 134.6, 134.4, 131.0, 130.1, 129.9, 129.5, 128.5, 128.3, 127.4, 125.7, 125.3, 122.6, 118.9, 114.2, 112.3, 110.8, 105.7, 55.5, 55.4$ ppm; HRMS: m/z calcd for C₂₇H₂₃N₄O₃ ([M+H]⁺) 451.1765, found 451.1761.

N-(3,4-Dimethoxyphenyl)-5-(4-methoxyphenyl)-1-(naphthalen-1-yl)-1*H*-1,2,4-triazole-3-carboxamide

(**5c**, C₂₈H₂₅N₄O₄)

Yellow crystals (229 mg, 55% yield); m.p.: 102–104 °C (methanol); IR (KBr): $\bar{\nu} = 3345$ (NH), 1695 (C=O), 1589 (C–N) cm⁻¹; ¹H NMR (400 MHz, CDCl₃): $\delta = 8.90$ (s, 1H, NH), 7.98 (d, $J = 8.2$ Hz, 1H, Ar-H), 7.91 (d, $J = 8.2$ Hz, 1H, Ar-H), 7.54–7.36 (m, 6H, Ar-H), 7.34 (d, $J = 8.8$ Hz, 2H, Ar-H), 7.15–7.06 (m, 1H, Ar-H), 6.80 (d, $J = 8.6$ Hz, 1H, Ar-H), 6.65 (d, $J = 8.8$ Hz, 2H, Ar-H), 3.84 (s, 3H, OCH₃), 3.82 (s, 3H, OCH₃), 3.66 (s, 3H, OCH₃) ppm; ¹³C NMR (101 MHz, CDCl₃): $\delta = 161.4, 156.9, 156.8, 149.3, 146.2, 134.6, 134.4, 131.3, 130.9, 130.1, 129.6, 128.5, 128.3, 127.4, 125.7, 125.3, 122.6, 118.9, 114.2, 112.1, 111.5, 104.9, 56.3, 56.1, 55.4$ ppm; HRMS: m/z calcd for C₂₈H₂₅N₄O₄ ([M+H]⁺) 481.1870, found 481.1867.

5-(4-Methoxyphenyl)-1-(naphthalen-1-yl)-*N*-(3,4,5-trimethoxyphenyl)-1*H*-1,2,4-triazole-3-carboxamide

(**5d**, C₂₉H₂₇N₄O₅)

Brown crystals (217 mg, 49% yield); m.p.: 100–102 °C (ethanol); IR (KBr): $\bar{\nu} = 3350$ (NH), 1691 (C=O), 1589

(C–N) cm^{-1} ; ^1H NMR (400 MHz, CDCl_3): δ = 8.96 (s, 1H, NH), 8.06 (d, J = 8.3 Hz, 1H, Ar–H), 7.98 (d, J = 8.3 Hz, 1H, Ar–H), 7.63–7.34 (m, 7H, Ar–H), 7.09 (s, 2H, Ar–H), 6.72 (d, J = 8.9 Hz, 2H, Ar–H), 3.89 (s, 6H, 2 \times OCH₃), 3.85 (s, 3H, OCH₃), 3.74 (s, 3H, OCH₃) ppm; ^{13}C NMR (101 MHz, CDCl_3): δ = 161.4, 157.0, 156.8, 153.5, 134.8, 134.4, 134.2, 133.6, 131.1, 130.1, 129.5, 128.5, 128.3, 127.4, 125.7, 125.3, 122.6, 118.9, 114.2, 97.8, 61.2, 56.3, 55.4 ppm; HRMS: m/z calcd for $\text{C}_{29}\text{H}_{27}\text{N}_4\text{O}_5$ ($[\text{M}+\text{H}]^+$) 511.1976, found 511.1976.

N-(3,5-Difluorophenyl)-5-(4-methoxyphenyl)-1-(naphthalen-1-yl)-1*H*-1,2,4-triazole-3-carboxamide

(**5e**, $\text{C}_{26}\text{H}_{19}\text{F}_2\text{N}_4\text{O}_2$)

Pale brown crystals (277 mg, 70% yield); m.p.: 94–96 °C (ethanol); IR (KBr): $\bar{\nu}$ = 3351 (NH), 1691 (C=O), 1589 (C–N) cm^{-1} ; ^1H NMR (400 MHz, CDCl_3): δ = 9.16 (s, 1H), 8.09 (d, J = 8.1 Hz, 1H, Ar–H), 8.01 (d, J = 8.1 Hz, 1H, Ar–H), 7.63–7.50 (m, 4H, Ar–H), 7.47–7.38 (m, 5H, Ar–H), 6.75 (d, J = 8.9 Hz, 2H, Ar–H), 6.69–6.59 (m, 1H, Ar–H), 3.77 (s, 3H, OCH₃) ppm; ^{13}C NMR (101 MHz, CDCl_3): δ = 164.7, 162.1, 161.8, 161.5, 157.1, 156.3, 134.3, 131.1, 130.1, 129.4, 128.6, 128.3, 127.5, 125.7, 125.3, 122.5, 118.7, 114.2, 103.3, 102.9, 99.9, 55.4 ppm; HRMS: m/z calcd for $\text{C}_{26}\text{H}_{19}\text{F}_2\text{N}_4\text{O}_2$ ($[\text{M} + \text{H}]^+$) 457.1471, found 457.1467.

5-(3,4-Dimethoxyphenyl)-*N*-(2-methoxyphenyl)-1-(naphthalen-1-yl)-1*H*-1,2,4-triazole-3-carboxamide

(**6a**, $\text{C}_{28}\text{H}_{25}\text{N}_4\text{O}_4$)

Red crystals (280 mg, 73% yield); m.p.: 99–101 °C (ethanol); IR (KBr): $\bar{\nu}$ = 3332 (NH), 1690 (C=O), 1589 (C–N) cm^{-1} ; ^1H NMR (400 MHz, CDCl_3): δ = 9.65 (s, 1H, NH), 8.64 (d, J = 7.9 Hz, 1H, Ar–H), 8.07 (d, J = 7.7 Hz, 1H, Ar–H), 8.00–7.93 (d, J = 7.8 Hz, 1H, Ar–H), 7.67–7.35 (m, 6H, Ar–H), 7.10–6.91 (m, 4H, Ar–H), 6.67 (d, J = 8.5 Hz, 1H, Ar–H), 3.93 (s, 3H, OCH₃), 3.80 (s, 3H, OCH₃), 3.46 (s, 3H, OCH₃) ppm; ^{13}C NMR (101 MHz, CDCl_3): δ = 148.7, 148.5, 134.3, 130.9, 128.4, 128.3, 127.4, 125.9, 125.4, 124.3, 122.7, 121.8, 121.3, 120.5, 111.3, 110.9, 110.1, 55.9, 55.6 ppm; HRMS: m/z calcd for $\text{C}_{28}\text{H}_{25}\text{N}_4\text{O}_4$ ($[\text{M} + \text{H}]^+$) 481.1870, found 481.1863.

5-(3,4-Dimethoxyphenyl)-*N*-(3-methoxyphenyl)-1-(naphthalen-1-yl)-1*H*-1,2,4-triazole-3-carboxamide

(**6b**, $\text{C}_{28}\text{H}_{25}\text{N}_4\text{O}_4$)

Yellow crystals (241 mg, 63% yield); m.p.: 121–123 °C (methanol); IR (KBr): $\bar{\nu}$ = 3336 (NH), 1696 (C=O), 1589 (C–N) cm^{-1} ; ^1H NMR (400 MHz, CDCl_3): δ = 9.02 (s, 1H, NH), 8.06 (d, J = 8.1 Hz, 1H, Ar–H), 7.98 (d, J = 8.1 Hz, 1H, Ar–H), 7.66–7.48 (m, 5H, Ar–H), 7.47–7.37 (m, 1H, Ar–H), 7.32–7.24 (m, 2H, Ar–H), 7.07–6.96 (m, 2H, Ar–H), 6.78–6.68 (m, 1H, Ar–H), 6.65

(d, J = 8.4 Hz, 1H, Ar–H), 3.84 (s, 3H, OCH₃), 3.79 (s, 3H, OCH₃), 3.47 (s, 3H, OCH₃) ppm; ^{13}C NMR (101 MHz, CDCl_3): δ = 160.2, 156.9, 156.8, 156.6, 150.7, 148.6, 138.5, 134.4, 134.1, 130.8, 129.7, 128.3, 128.2, 127.5, 125.5, 125.1, 122.3, 121.6, 118.8, 111.9, 111.1, 110.8, 110.6, 105.6, 56.1, 55.7, 55.5 ppm; HRMS: m/z calcd for $\text{C}_{28}\text{H}_{25}\text{N}_4\text{O}_4$ ($[\text{M}+\text{H}]^+$) 481.1870, found 481.1862.

N,5-Bis(3,4-dimethoxyphenyl)-1-(naphthalen-1-yl)-1*H*-1,2,4-triazole-3-carboxamide (**6c**, $\text{C}_{29}\text{H}_{27}\text{N}_4\text{O}_5$)

Red crystals (265 mg, 65% yield); m.p.: 89–91 °C (methanol); ^1H NMR (400 MHz, CDCl_3): δ = 8.94 (s, 1H, NH), 8.07 (d, J = 8.1 Hz, 1H, Ar–H), 7.98 (d, J = 8.1 Hz, 1H, Ar–H), 7.63–7.41 (m, 6H, Ar–H), 7.18 (dd, J = 8.6, 2.5 Hz, 1H, Ar–H), 7.07–6.98 (m, 2H, Ar–H), 6.87 (d, J = 8.7 Hz, 1H, Ar–H), 6.66 (d, J = 8.4 Hz, 1H, Ar–H), 3.93 (s, 3H, OCH₃), 3.89 (s, 3H, OCH₃), 3.80 (s, 3H, OCH₃), 3.48 (s, 3H, OCH₃) ppm; ^{13}C NMR (101 MHz, CDCl_3): δ = 156.9, 150.9, 149.3, 148.8, 146.2, 134.8, 134.4, 131.2, 130.9, 129.7, 128.5, 128.4, 127.5, 125.8, 125.4, 122.6, 121.8, 118.9, 112.1, 111.5, 111.2, 110.9, 104.9, 56.3, 56.2, 56.1, 55.7 ppm; HRMS: m/z calcd for $\text{C}_{29}\text{H}_{27}\text{N}_4\text{O}_5$ ($[\text{M}+\text{H}]^+$) 511.1976, found 511.1971.

5-(3,4-Dimethoxyphenyl)-1-(naphthalen-1-yl)-*N*-(3,4,5-trimethoxyphenyl)-1*H*-1,2,4-triazole-3-carboxamide

(**6d**, $\text{C}_{30}\text{H}_{29}\text{N}_4\text{O}_6$)

Pale brown crystals (237 mg, 55% yield); m.p.: 94–96 °C (methanol); ^1H NMR (400 MHz, CDCl_3): δ = 8.94 (s, 1H, NH), 8.06 (d, J = 8.1 Hz, 1H, Ar–H), 7.98 (d, J = 8.1 Hz, 1H, Ar–H), 7.73–7.38 (m, 5H, Ar–H), 7.08 (s, 2H, Ar–H), 7.06–6.83 (m, 2H, Ar–H), 6.66 (d, J = 8.4 Hz, 1H, Ar–H), 3.89 (s, 6H, 2OCH₃), 3.84 (s, 3H, OCH₃), 3.80 (s, 3H, OCH₃), 3.47 (s, 3H, OCH₃) ppm; ^{13}C NMR (101 MHz, CDCl_3): δ = 157.1, 157.1, 156.8, 153.5, 150.9, 148.8, 135.1, 134.7, 134.4, 133.7, 131.1, 129.6, 128.5, 128.4, 127.5, 125.8, 125.4, 122.5, 121.8, 118.8, 111.2, 110.9, 97.8, 61.1, 56.3, 56.1, 55.7 ppm; HRMS: m/z calcd for $\text{C}_{30}\text{H}_{29}\text{N}_4\text{O}_6$ ($[\text{M}+\text{H}]^+$) 541.2082, found 541.2100.

N-(3,5-Difluorophenyl)-5-(3,4-dimethoxyphenyl)-1-(naphthalen-1-yl)-1*H*-1,2,4-triazole-3-carboxamide

(**6e**, $\text{C}_{27}\text{H}_{21}\text{F}_2\text{N}_4\text{O}_3$)

Brown crystals (264 mg, 68% yield); m.p.: 91–93 °C (ethanol); ^1H NMR (400 MHz, CDCl_3): δ = 9.21 (s, 1H, NH), 8.07 (d, J = 8.1 Hz, 1H, Ar–H), 7.98 (d, J = 8.2 Hz, 1H, Ar–H), 7.74–7.28 (m, 7H, Ar–H), 7.12–6.87 (m, 2H, Ar–H), 6.73–6.54 (m, 2H, Ar–H), 3.79 (s, 3H, OCH₃), 3.47 (s, 3H, OCH₃) ppm; ^{13}C NMR (101 MHz, CDCl_3): δ = 164.5, 164.3, 162.1, 161.9, 151.1, 148.7, 139.8, 134.2, 131.0, 129.3, 128.4, 128.3, 127.4, 125.7, 125.2,

122.2, 121.8, 111.1, 110.8, 103.2, 102.9, 99.9, 56.0, 55.7 ppm; HRMS: m/z calcd for $C_{27}H_{21}F_2N_4O_3$ ($[M+H]^+$) 487.1576, found 487.1571.

N-(2-Methoxyphenyl)-1-(naphthalen-1-yl)-5-(3,4,5-trimethoxyphenyl)-1*H*-1,2,4-triazole-3-carboxamide (7a, $C_{29}H_{27}N_4O_5$)

Orange crystals (245 mg, 65% yield); m.p.: 94–96 °C (methanol); 1H NMR (400 MHz, $CDCl_3$): δ = 9.72 (s, 1H, NH), 8.71 (d, J = 8.1 Hz, 1H, Ar–H), 8.07 (d, J = 8.1 Hz, 1H, Ar–H), 8.00 (d, J = 8.1 Hz, 1H, Ar–H), 7.74–7.48 (m, 4H, Ar–H), 7.49–7.39 (m, 1H, Ar–H), 7.19–7.00 (m, 2H, Ar–H), 6.95 (d, J = 7.2 Hz, 1H, Ar–H), 6.81 (s, 2H, Ar–H), 3.84 (s, 3H, OCH_3), 3.80 (s, 3H, OCH_3), 3.51 (s, 6H, $2 \times OCH_3$) ppm; ^{13}C NMR (101 MHz, $CDCl_3$): δ = 156.9, 156.7, 156.6, 152.9, 148.3, 139.8, 134.7, 134.1, 130.8, 129.6, 128.4, 128.3, 127.4, 127.2, 125.9, 125.3, 124.3, 122.4, 121.2, 120.3, 60.9, 55.8, 55.4 ppm; HRMS: m/z calcd for $C_{29}H_{27}N_4O_5$ ($[M+H]^+$) 511.1976, found 512.2054.

N-(3-Methoxyphenyl)-1-(naphthalen-1-yl)-5-(3,4,5-trimethoxyphenyl)-1*H*-1,2,4-triazole-3-carboxamide (7b, $C_{29}H_{27}N_4O_5$)

Yellow crystals (279 mg, 74% yield); m.p.: 110–112 °C (methanol); 1H NMR (400 MHz, $CDCl_3$): δ = 9.10 (s, 1H, NH), 8.05 (d, J = 8.1 Hz, 1H, Ar–H), 7.96 (d, J = 8.1 Hz, 1H, Ar–H), 7.70–7.43 (m, 5H, Ar–H), 7.46–7.29 (m, 2H, Ar–H), 7.30–7.17 (m, 2H, Ar–H), 6.69 (s, 2H, Ar–H), 3.82 (s, 3H, OCH_3), 3.76 (s, 3H, OCH_3), 3.39 (s, 6H, $2 \times OCH_3$) ppm; ^{13}C NMR (101 MHz, $CDCl_3$): δ = 160.1, 156.5, 156.2, 153.2, 140.1, 138.4, 134.6, 134.1, 130.9, 129.8, 129.5, 128.5, 128.4, 127.3, 125.6, 125.1, 122.1, 120.8, 112.1, 110.6, 105.6, 60.9, 55.9, 55.5 ppm; HRMS: m/z calcd for $C_{29}H_{27}N_4O_5$ ($[M+H]^+$) 511.1976, found 511.1971.

N-(3,4-Dimethoxyphenyl)-1-(naphthalen-1-yl)-5-(3,4,5-trimethoxyphenyl)-1*H*-1,2,4-triazole-3-carboxamide (7c, $C_{30}H_{29}N_4O_6$)

Yellow crystals (240 mg, 60% yield); m.p.: 105–107 °C (ethanol); 1H NMR (400 MHz, $CDCl_3$): δ = 9.11 (s, 1H, NH), 8.07 (d, J = 8.1 Hz, 1H, Ar–H), 7.98 (d, J = 8.2 Hz, 1H, Ar–H), 7.64–7.49 (m, 5H, Ar–H), 7.42 (d, J = 8.3 Hz, 1H, Ar–H), 7.20 (dd, J = 8.6, 2.3 Hz, 1H, Ar–H), 6.86 (d, J = 8.6 Hz, 1H, Ar–H), 6.71 (s, 2H, Ar–H), 3.92 (s, 3H, OCH_3), 3.88 (s, 3H, OCH_3), 3.77 (s, 3H, OCH_3), 3.41 (s, 6H, $2 \times OCH_3$) ppm; ^{13}C NMR (101 MHz, $CDCl_3$): δ = 156.4, 156.2, 153.1, 149.1, 146.1, 140.1, 134.3, 134.1, 130.9, 129.4, 128.5, 128.3, 127.3, 125.3, 122.2, 112.1, 111.4, 105.7, 105.6, 104.8, 60.9, 56.2, 56.1, 55.9 ppm; HRMS: m/z calcd for $C_{30}H_{29}N_4O_6$ ($[M+H]^+$) 541.2082, found 541.2075.

1-(Naphthalen-1-yl)-*N*,5-bis(3,4,5-trimethoxyphenyl)-1*H*-1,2,4-triazole-3-carboxamide (7d, $C_{31}H_{31}N_4O_7$)

Brown crystals (245 mg, 58% yield); m.p.: 113–115 °C (ethanol); 1H NMR (400 MHz, $CDCl_3$): δ = 8.95 (s, 1H, NH), 8.20 (s, 1H, Ar–H), 8.08 (d, J = 7.8 Hz, 1H, Ar–H), 7.99 (d, J = 7.9 Hz, 1H, Ar–H), 7.62–7.50 (m, 3H, Ar–H), 7.44 (d, J = 8.1 Hz, 1H, Ar–H), 7.09 (s, 2H, Ar–H), 6.69 (s, 2H, Ar–H), 3.89 (s, 6H, $2 \times OCH_3$), 3.85 (s, 3H, OCH_3), 3.78 (s, 3H, OCH_3), 3.42 (s, 6H, $2 \times OCH_3$) ppm; ^{13}C NMR (101 MHz, $CDCl_3$): δ = 153.5, 153.1, 152.8, 139.7, 134.9, 134.4, 134.1, 133.2, 130.9, 129.3, 128.5, 128.4, 127.5, 127.3, 125.9, 125.1, 122.2, 122.1, 105.5, 97.6, 61.1, 60.7, 56.2, 55.7 ppm; HRMS: m/z calcd for $C_{31}H_{31}N_4O_7$ ($[M+H]^+$) 571.2187, found 571.2183.

N-(3,5-Difluorophenyl)-1-(naphthalen-1-yl)-5-(3,4,5-trimethoxyphenyl)-1*H*-1,2,4-triazole-3-carboxamide (7e, $C_{28}H_{23}F_2N_4O_4$)

Yellow crystals (210 mg, 55% yield); m.p.: 100–102 °C (ethanol); 1H NMR (400 MHz, $CDCl_3$): δ = 9.18 (s, 1H, NH), 8.07 (d, J = 8.2 Hz, 1H, Ar–H), 7.98 (d, J = 8.2 Hz, 1H, Ar–H), 7.76–7.45 (m, 5H, Ar–H), 7.44–7.36 (m, 2H, Ar–H), 6.68 (s, 2H, Ar–H), 6.64–6.56 (m, 1H, Ar–H), 3.77 (s, 3H, OCH_3), 3.41 (s, 6H, $2 \times OCH_3$) ppm; ^{13}C NMR (101 MHz, $CDCl_3$): δ = 164.4, 162.1, 161.7, 156.6, 155.7, 153.3, 140.1, 139.4, 134.1, 130.8, 129.2, 128.3, 127.5, 125.5, 125.1, 122.2, 120.6, 105.4, 103.2, 102.5, 99.9, 60.9, 55.8 ppm; HRMS: m/z calcd for $C_{28}H_{23}F_2N_4O_4$ ($[M+H]^+$) 517.1682, found 517.1679.

N-(2-Methoxybenzyl)-1-(naphthalen-1-yl)-5-(3,4,5-trimethoxyphenyl)-1*H*-1,2,4-triazole-3-carboxamide (7f, $C_{30}H_{29}N_4O_5$)

Brown crystals (205 mg, 53% yield); m.p.: 70–71 °C (ethyl acetate/*n*-hexane 8:2); 1H NMR (400 MHz, $CDCl_3$): δ = 8.04 (d, J = 8.3 Hz, 1H, Ar–H), 7.95 (d, J = 8.0 Hz, 1H, Ar–H), 7.81 (s, 1H, Ar–H), 7.65–7.48 (m, 4H, Ar–H), 7.43–7.37 (m, 2H, Ar–H), 7.31–7.25 (m, 1H, Ar–H), 6.99–6.84 (m, 1H, Ar–H), 6.67 (s, 2H, Ar–H), 4.74 (d, J = 6.0 Hz, 2H, $NHCH_2$), 3.87 (s, 3H, OCH_3), 3.75 (s, 3H, OCH_3), 3.38 (s, 6H, $2 \times OCH_3$) ppm; ^{13}C NMR (101 MHz, $CDCl_3$): δ = 158.7, 157.8, 153.1, 139.9, 136.6, 134.7, 134.2, 130.9, 130.1, 129.7, 129.1, 128.5, 128.4, 127.5, 125.9, 125.4, 122.4, 120.8, 110.5, 105.8, 60.9, 55.8, 55.5, 39.2 ppm; HRMS: m/z calcd for $C_{30}H_{29}N_4O_5$ ($[M+H]^+$) 525.2132, found 525.2127.

N-(3-Methoxybenzyl)-1-(naphthalen-1-yl)-5-(3,4,5-trimethoxyphenyl)-1*H*-1,2,4-triazole-3-carboxamide (7g, $C_{30}H_{29}N_4O_5$)

Brown crystals (232 mg, 60% yield); m.p.: 89–90 °C (ethyl acetate/*n*-hexane 9:1); 1H NMR (400 MHz, $CDCl_3$): δ = 8.05 (d, J = 8.1 Hz, 1H, Ar–H), 7.96 (d, J = 8.1 Hz, 1H, Ar–H), 7.60–7.49 (m, 4H, Ar–H), 7.40 (d, J = 8.2 Hz,

1H, Ar-H), 7.33–7.27 (m, 1H, Ar-H), 6.99–7.09 (m, 2H, Ar-H), 6.85–6.80 (m, 1H, Ar-H), 6.66 (s, 2H, Ar-H), 4.71 (d, $J = 5.9$ Hz, 2H, NHCH₂), 3.81 (s, 3H, OCH₃), 3.76 (s, 3H, OCH₃), 3.39 (s, 6H, 2×OCH₃) ppm; ¹³C NMR (101 MHz, CDCl₃): $\delta = 153.1, 147.6, 134.5, 134.2, 133.6, 130.9, 129.9, 129.7, 128.5, 128.4, 127.5, 125.9, 125.4, 124.3, 122.5, 121.3, 120.5, 113.9, 113.3, 105.7, 60.9, 55.8, 55.5, 43.7$ ppm; HRMS: m/z calcd for C₃₀H₂₉N₄O₅ ([M+H]⁺) 525.2132, found 525.2128.

N-(3,4-Dimethoxybenzyl)-1-(naphthalen-1-yl)-5-(3,4,5-trimethoxyphenyl)-1H-1,2,4-triazole-3-carboxamide (7h, C₃₁H₃₁N₄O₆)

Pale brown crystals (254 mg, 62% yield); m.p.: 89–90 °C (ethyl acetate/*n*-hexane 7:3); ¹H NMR (400 MHz, CDCl₃): $\delta = 8.06$ (d, $J = 8.1$ Hz, 1H, Ar-H), 7.98–7.92 (d, $J = 8.1$ Hz, 1H, Ar-H), 7.85–7.76 (m, 1H, Ar-H), 7.62–7.47 (m, 4H, Ar-H), 7.39 (t, $J = 4.4$ Hz, 1H, Ar-H), 6.99–6.94 (m, 1H, Ar-H), 6.84 (d, $J = 8.1$ Hz, 1H, Ar-H), 6.68 (s, 2H, Ar-H), 4.67 (d, $J = 5.8$ Hz, 2H, NHCH₂), 3.90 (s, 3H, OCH₃), 3.87 (s, 3H, OCH₃), 3.76 (s, 3H, OCH₃), 3.39 (s, 6H, 2×OCH₃) ppm; ¹³C NMR (101 MHz, CDCl₃): $\delta = 153.1, 149.3, 148.8, 134.2, 131.1, 130.5, 129.6, 128.6, 128.5, 127.6, 125.9, 125.4, 122.3, 120.8, 111.9, 111.3, 105.9, 60.9, 56.1, 56.1, 55.9, 43.6$ ppm; HRMS: m/z calcd for C₃₁H₃₁N₄O₆ ([M+H]⁺) 555.2238, found 555.2232.

N-(3,5-Difluorobenzyl)-1-(naphthalen-1-yl)-5-(3,4,5-trimethoxyphenyl)-1H-1,2,4-triazole-3-carboxamide (7i, C₂₉H₂₅F₂N₄O₄)

Yellow crystals (270 mg, 69% yield); m.p.: 75–77 °C (ethyl acetate/*n*-hexane 8:2); ¹H NMR (400 MHz, CDCl₃): $\delta = 8.06$ (d, $J = 8.1$ Hz, 1H, Ar-H), 7.96 (d, $J = 8.1$ Hz, 1H, Ar-H), 7.73 (s, 1H, Ar-H), 7.59–7.52 (m, 4H, Ar-H), 7.41 (d, $J = 8.3$ Hz, 1H, Ar-H), 6.94 (s, 1H, Ar-H), 6.75–6.70 (m, 1H, Ar-H), 6.67 (s, 2H, Ar-H), 4.71 (d, $J = 6.2$ Hz, 2H, -NHCH₂), 3.76 (s, 3H, OCH₃), 3.39 (s, 6H, 2×OCH₃) ppm; ¹³C NMR (101 MHz, CDCl₃): $\delta = 164.5, 161.9, 159.3, 156.7, 153.1, 139.9, 134.6, 131.0, 129.6, 128.5, 127.6, 125.9, 125.4, 122.4, 121.1, 110.9, 110.6, 105.7, 103.1, 102.9, 60.9, 55.8, 42.7$ ppm; HRMS: m/z calcd for C₂₉H₂₅F₂N₄O₄ ([M+H]⁺) 531.1838, found 531.1837.

N-(3-Methylbenzyl)-1-(naphthalen-1-yl)-5-(3,4,5-trimethoxyphenyl)-1H-1,2,4-triazole-3-carboxamide (7j, C₃₀H₂₉N₄O₄)

Yellow crystals (271 mg, 72% yield); m.p.: 98–100 °C (ethyl acetate/*n*-hexane 7:3); ¹H NMR (400 MHz, CDCl₃): $\delta = 7.67$ (d, $J = 8.1$ Hz, 1H, Ar-H), 7.59 (d, $J = 8.1$ Hz, 1H, Ar-H), 7.33 (s, 1H, Ar-H), 7.24–7.15 (m, 2H, Ar-H), 7.12 (s, 1H, Ar-H), 7.02 (d, $J = 8.3$ Hz, 1H, Ar-H), 6.95–6.78 (m, 3H, Ar-H), 6.74 (d, $J = 7.2$ Hz, 1H, Ar-H),

6.29 (s, 2H, Ar-H), 4.33 (d, $J = 5.9$ Hz, 2H, NHCH₂), 3.38 (s, 3H, OCH₃), 3.01 (s, 6H, 2×OCH₃), 1.98 (s, 3H, CH₃) ppm; ¹³C NMR (101 MHz, CDCl₃): $\delta = 158.9, 156.3, 153.1, 140.0, 138.6, 137.8, 134.6, 134.2, 130.9, 129.6, 129.1, 128.7, 128.5, 128.5, 128.4, 127.5, 125.9, 125.4, 125.3, 122.4, 120.9, 105.8, 60.9, 55.8, 43.7, 21.5$ ppm; HRMS: m/z calcd for C₃₀H₂₉N₄O₄ ([M+H]⁺) 509.2183, found 509.2177.

N-Benzyl-1-(naphthalen-1-yl)-5-(3,4,5-trimethoxyphenyl)-1H-1,2,4-triazole-3-carboxamide (7k, C₂₉H₂₇N₄O₄)

Brown crystals (260 mg, 71% yield); m.p.: 86–88 °C (ethyl acetate/*n*-hexane 8:2); ¹H NMR (400 MHz, CDCl₃): $\delta = 8.04$ (d, $J = 8.1$ Hz, 1H, Ar-H), 7.95 (d, $J = 8.0$ Hz, 1H, Ar-H), 7.70 (s, 1H, Ar-H), 7.60–7.52 (m, 2H, Ar-H), 7.49 (s, 1H, Ar-H), 7.45–7.21 (m, 6H, Ar-H), 6.65 (s, 2H, Ar-H), 4.73 (d, $J = 5.7$ Hz, 2H, NHCH₂), 3.75 (s, 3H, OCH₃), 3.37 (s, 6H, 2×OCH₃) ppm; ¹³C NMR (101 MHz, CDCl₃): $\delta = 158.9, 156.4, 153.1, 139.9, 137.9, 134.6, 134.2, 130.9, 129.5, 128.7, 128.3, 128.2, 127.7, 127.4, 125.9, 125.4, 122.4, 121.0, 105.7, 60.9, 55.8, 43.7$ ppm; HRMS: m/z calcd for C₂₉H₂₇N₄O₄ ([M+H]⁺) 495.2027, found 495.2021.

Cell culture

Human hepatocarcinoma cell line (Hep-G2) and leukemia (HL-60), which were purchased from ATCC, USA, were used to evaluate the cytotoxic effect of the tested samples. Cells were routinely cultured in Dulbecco's modified Eagle's medium (DMEM). Medium was supplemented with 10% fetal bovine serum (FBS), 2 mM glutamine, containing 100 units/cm³ of penicillin G sodium, 100 units/cm³ of streptomycin sulfate, and 250 ng/cm³ amphotericin B. Cells were maintained at sub-confluence at 37 °C in humidified air containing 5% CO₂. For sub-culturing, monolayer cells were harvested after trypsin/EDTA treatment at 37 °C. Cells were used when confluence had reached 75%. Tested samples were dissolved in dimethyl sulfoxide (DMSO), and then diluted thousand times in the assay to begin with the indicated concentration. All cell culture material was obtained from Cambrex BioScience (Copenhagen, Denmark). All chemicals were from Sigma/Aldrich (USA), except mentioned. All experiments were repeated three times, unless mentioned.

Antitumor activity

Cytotoxicity of tested samples was measured against each cell line using the MTT cell viability assay. MTT (3-(4,5-dimethylthiazole-2-yl)-2,5-diphenyltetrazolium bromide) assay is based on the ability of active mitochondrial dehydrogenase enzyme of living cells to cleave the

tetrazolium rings of the yellow MTT and form a dark blue, insoluble formazan crystal, which is largely impermeable to cell membranes, resulting in its accumulation within healthy cells. Solubilization of the cells results in the liberation of crystals, which are then solubilized. The number of viable cells is directly proportional to the level of soluble formazan dark blue color. The extent of the reduction of MTT was quantified by measuring the absorbance at 570 nm.

Briefly, cells (0.5×10^5 cells/well), in serum-free media, were plated in a flat-bottom 96-well microplate, and treated with 20 cm^3 of serial concentrations of the tested samples for 48 h at 37°C in a humidified 5% CO_2 atmosphere. After incubation, media were removed and 40 cm^3 of MTT solution (5 mg/cm^3 of MTT in 0.9% NaCl) in each well was added and incubated for an additional 4 h. MTT crystals were solubilized by adding 180 cm^3 of acidified isopropanol/well and the plate was shaken at room temperature, followed by photometric determination of the absorbance at 570 nm using microplate ELISA reader. Triplicate repeats were performed for each concentration and the average was calculated. Data were expressed as the percentage of relative viability compared with the untreated cells compared with the vehicle control, with cytotoxicity indicated by $<100\%$ relative viability. Percentage of relative viability was calculated using the following equation: $[\text{absorbance of treated cells}/\text{absorbance of control cells}] \times 100$. Then, the half maximal inhibitory concentration (IC_{50}) was calculated from the equation of the dose–response curve (linear regression), with drug concentrations x_1, x_2, \dots, x_n and growth inhibition y_1, y_2, \dots, y_n .

Immunofluorohistochemical evaluation of tubulin

Immunohistochemical detection of tubulin in fixed cells was followed according to the method originally developed by Kawahira, with some modifications.

Reagents preparation: 0.1 M citrate buffer pH to 6.0: 9 cm^3 of 0.1 M citric acid solution was added to 41 cm^3 of 1 M sodium citrate solution and the volume was adjusted to 500 cm^3 by deionized water. Antigen retrieval solution: 50 cm^3 of 0.1 M citrate buffer, 500 cm^3 of Triton-100, and 250 cm^3 of Tween-20 were mixed together and the final volume was adjusted to 500 cm^3 by deionized water. Blocking solution: 50 cm^3 of 0.1 M citrate buffer, 500 cm^3 of Triton-100, 250 cm^3 of Tween-20, and 25 cm^3 of FBS were mixed together and the final volume was adjusted to 500 cm^3 by deionized water.

Procedure: Slides of fixed cells were rinsed in three changes of PBS. Antigen retrieval step, by which the availability of the antigen for interaction with a specific antibody is maximized, was performed by immersing slides in antigen retrieval solution and then incubating in a water

bath at $95\text{--}99^\circ\text{C}$ for 20 min. Afterwards, slides were directly transferred to pre-cooled antigen retrieval solution placed at 4°C for 5 min. Non-specific binding of the antibody is prevented by incubating the slides in blocking solution at 37°C for 30 min. Slides were then incubated for 30 min at 37°C with rabbit anti-human tubulin antibody (1:500) diluted with blocking solution. Excess antiserum was rinsed from the slide by immersing in cold buffer for two changes of 5–10 min each. Slides were then incubated at 37°C with goat FITC anti-rabbit IgG (1:2500) diluted with blocking solution. The slides were rinsed in the enzyme substrate till the color developed. Images were visualized using a fluorescence microscope (Axiostar Plus, Zeiss, Goettingen, Germany) equipped with image analyzer and digital camera (PowerShot A20, Canon, USA).

Cell-cycle analysis

Hep-G2 cells (5×10^5) were collected after being treated with the tested compounds, washed twice with PBS, re-suspended in 250 mm^3 of PBS and mixed with 4 cm^3 of ice-cold 70% ethanol. The cells were centrifuged and the pellets were re-suspended in 1 cm^3 of propidium iodide (PI)/Triton X-100 staining solution (0.1% Triton X-100 in PBS, 0.2 mg/cm^3 RNase A and $10 \mu\text{g/cm}^3$ PI) and incubated for 30 min at room temperature. The stained cells were analyzed by flow cytometry.

Docking of the target molecules to tubulin protein in colchicine-binding site

Molecular modeling studies were performed using Molecular Operating Environment (MOE[®]) version 2014.09 programs. The ligands were built using the builder tool of MOE[®] and subjected to energy minimization using MMFF94x force field. The X-ray crystallographic structure of tubulin complexed with DAMA-colchicine was obtained from the Protein Data Bank through the Internet (<http://www.rcsb.org/>, PDB code 1SA0) [15]. The errors of the protein were corrected. Essential hydrogen atoms and Kollman united atom type charges were added with the aid of MOE[®] tools. Affinity (grid) maps of $20 \times 20 \times 20 \text{ \AA}$ grid points and 0.375 \AA spacing were generated using the AutoGrid program [16]. MOE[®] parameter set and distance-dependent dielectric functions were used in the calculation of the van der Waals and the electrostatic terms, respectively. Docking simulations were performed using the Lamarckian genetic algorithm (LGA) and the Solis & Wets local search method [17]. Initial position, orientation, and torsions of the ligand molecules were set randomly. Each docking experiment was derived from 10 different runs that were set to terminate after a maximum of 250,000 energy evaluations. The population size was set to 150. During the

search, a translational step of 0.2 Å, and quaternion and torsion steps of 5 were applied [18–20].

Acknowledgements This work was financially supported by the Science and Technology Development Fund (STDF) of Egypt (Project No. 2943 Basic and Applied Research). Moreover, all eternal thanks to the National Cancer Institute (NCI), Bethesda, Maryland, USA, for performing the anticancer testing of the target compounds over 60 cancer cell lines. Finally, we would like to thank Prof. Amira M. Gamal-Eldeen, Cancer Biology Laboratory, Center of Excellence for Advanced Sciences, National Research Center, Cairo, Egypt, for her help in studying the cytotoxicity of the synthesized compounds.

References

- Jordan MA, Wilson L (2004) *Nat Rev Cancer* 4:253
- Thomson P, Naylor MA, Everett SA, Stratford MRL, Lewis G, Hill S, Patel KB, Wardman P, Davis PD (2006) *Mol Cancer Ther* 5:2886
- Mikstacka R, Stefanski T, Rozanski J (2013) *Cell Mol Biol Lett* 18:368
- Tozer GM, Kanthou C, Parkins CS, Hill SA (2002) *Int J Exp Pathol* 83:21
- Pettit GR, Singh SB, Hamel E, Lin CM, Alberts DS, Garcia-Kendal D (1989) *Experientia* 45:209
- Pettit GR, Singh SB, Niven ML, Hamel E, Schmidt JM (1987) *J Nat Prod* 50:119
- Hsieh HP, Liou JP, Mahindroo N (2005) *Curr Pharm Des* 11:1655
- Zhang Q, Peng Y, Wang XI, Keenan SM, Arora S, Welshet WJ (2007) *J Med Chem* 50:749
- Pati HN, Wicks M, Holt HL, Leblanc R, Weisbruch P, Forrest L, Lee M (2005) *Heterocycl Commun* 11:117
- Gaukroger K, Hadfield JA, Lawrence NJ, Nolan S, McGown AT (2003) *Org Biomol Chem* 1:3033
- Pettit GR, Minardi MD, Rosenberg HJ, Hamel E, Bibby MC, Martin SW, Jung MK, Pettit RK, Cuthbertson TJ, Chapuis JC (2005) *J Nat Prod* 68:1450
- Acheson RM, Booth DA, Brettle R, Harris AM (1960) *J Chem Soc* 694:3457
- Aly OM, Beshr EA, Maklad RM, Mustafa M, Gamal-Eldeen AM (2014) *Arch Pharm Chem Life Sci* 347:1
- Al-Ghamdi RF (2005) *J Saudi Chem Soc* 9:391
- Ravelli RB, Gigant B, Curmi PA, Jourdain I, Lachkar S, Sobel A, Knossow M (2004) *Nature* 428:198
- Morris GM, Goodsell DS, Halliday RS, Huey R, Hart WE, Belew RK, Olson AJ (1998) *J Comput Chem* 19:1639
- Solis FJ, Wets RJB (1981) *Math Oper Res* 6:19
- Bikadi Z, Demko L, Hazai E (2007) *Arch Biochem Biophys* 461:225
- McDonald IK, Thornton JM (1994) *J Mol Biol* 238:777
- Humphrey W, Dalke A, Schulten K (1996) *J Mol Gr* 14:33